28
11-6-81

B8170

ornl

OAK
RIDGE
NATIONAL
LABORATORY

UNION
CARBIDE

OPERATED BY
UNION CARBIDE CORPORATION
FOR THE UNITED STATES
DEPARTMENT OF ENERGY

ORNL/TM-7972

MASTER

Monte Carlo Analysis of a Time-Dependent Neutron and Secondary Gamma-Ray Integral Experiment on a Thick Concrete and Steel Shield

S. N. Cramer
R. W. Roussin

Printed in the United States of America Available from
National Technical Information Service
U.S. Department of Commerce
5285 Port Royal Road, Springfield, Virginia 22161
NTIS price codes—Printed Copy: A03; Microfiche A01

ORNL/TM-7972

Contract No. W-7405-eng-26

Engineering Physics Division

MONTE CARLO ANALYSIS OF A TIME-DEPENDENT NEUTRON AND SECONDARY GAMMA-RAY INTEGRAL EXPERIMENT ON A THICK CONCRETE AND STEEL SHIELD

S. N. Cramer
R. W. Roussin

Date Published - November 1981

Work Sponsored by
Defense Nuclear Agency
Under Subtask No. V99QAXNA

OAK RIDGE NATIONAL LABORATORY
Oak Ridge, Tennessee 37830
operated by
UNION CARBIDE CORPORATION
for the
DEPARTMENT OF ENERGY

TABLE OF CONTENTS

ABSTRACT

A Monte Carlo analysis of a time-dependent neutron and secondary gamma-ray integral experiment on a thick concrete and steel shield is presented. The energy range covered in the analysis is 15-2 MeV for neutron source energies. The multigroup MORSE code was used with the VITAMIN C 171-36 neutron-gamma-ray cross-section data set. Both neutron and gamma-ray count rates and unfolded energy spectra are presented and compared, with good general agreement, with experimental results.

I. INTRODUCTION

A Monte Carlo calculational analysis of a time-dependent neutron and secondary-gamma-ray integral experiment on a thick concrete and steel shield is presented here. The details of the experiment and measured data are given in reference 1. The analysis was performed with the MORSE multigroup Monte Carlo code,[2] and the cross section data set used was the 171-36 neutron-gamma-ray VITAMIN-C library.[3] The energy range of the analysis is 15-2 MeV. The shield is a concrete and steel layered slab 88.42-cm thick. A pulsed-white-neutron source from an electron linear accelerator was incident on the front face of the shield and the measurements were made with an NE-213 detector placed behind the shield. Both neutron and gamma ray count rates and unfolded energy spectra were calculated and compared with the measured results. Some conclusions are drawn and additional insight is developed by comparison with a previous analysis with the continuous energy TRIPOLI Monte Carlo code,[4] which considered only neutron calculational results.

II. CALCULATIONAL MODEL OF THE EXPERIMENT

The general experimental setup as described in reference 1 is shown schematically in Fig. 1. Neutrons are produced in the source at time zero with a spectrum covering the energy range 20 MeV to thermal. These neutrons travel down the flight path and strike the leading edge of the sample, shown in detail in Fig. 2. The eight concrete and fifteen steel slabs are 182.9 cm x 182.9 cm rectangles with the indicated thicknesses. In the calculation the detector was modeled as a point located at the

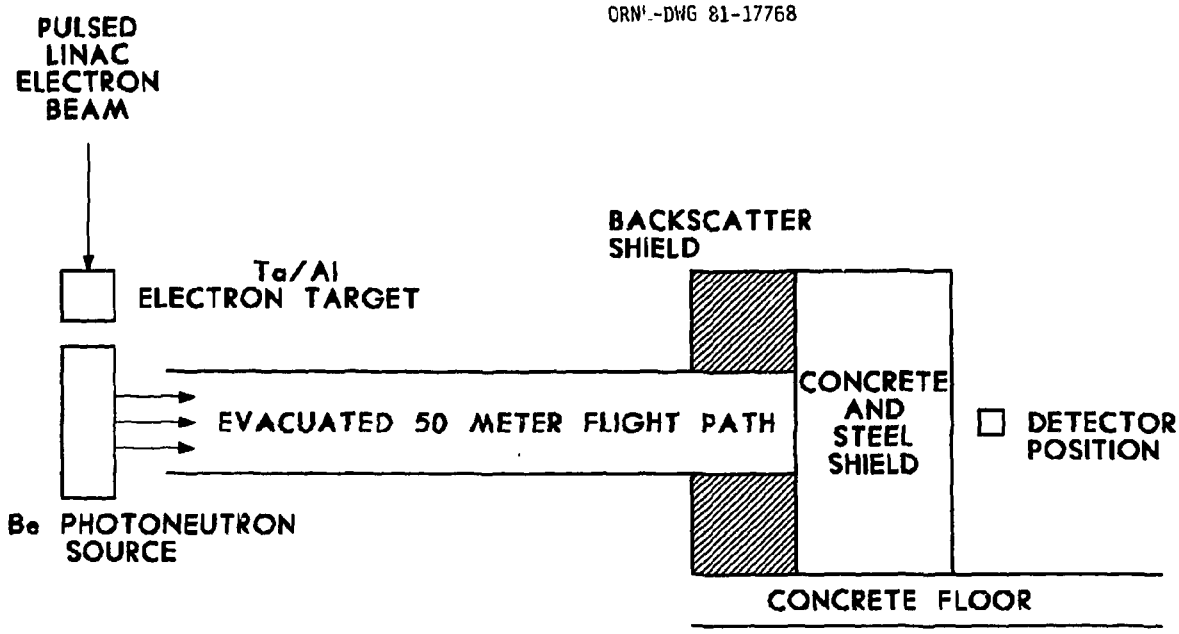

Fig. 1. Experimental Configuration.

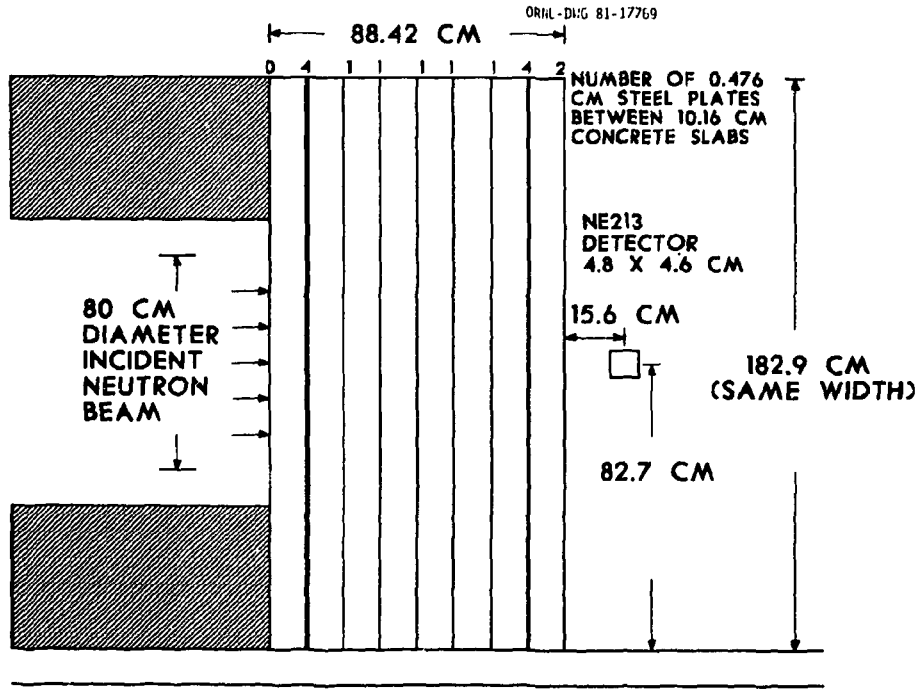

Fig. 2. Details of the Concrete and Steel Shield.
(NOT TO SCALE)

center of the experimental detector position as indicated and mid-way between the left and right edges. Vacuum boundary conditions were used at the leading edge and top of the sample, under the concrete floor, and two meters beyond the back edge. The source for the calculation was a uniform 80-cm-diameter circular disk with initial directions perpendicular to the front edge. The initial time distribution for the particle histories was determined from the time-energy relationship of the neutrons traveling down the 51.645 meter flight path. The initial energies were determined from a portion of the experimental source spectrum given in Table 1.

The cross section energy group structure for the 171-36 group VITAMIN-C, P_3 expansion data set is shown in Table 2. Also given in this table are the neutron and gamma-ray response functions and the neutron induced gamma-ray counts for the NE-213 detector as provided in reference 1 and fitted to the cross-section group structure. The nuclide concentrations for the concrete and steel compositions are given in Table 3.

III. DETAILS OF THE CALCULATION

Several modifications were made to the standard MORSE code for the purpose of these calculations. Initial energies and energy groups were determined from a distribution from Table 1 in a special SOURCE subroutine. In this routine the initial age of each particle was determined relativistically from the chosen energy and the flight path distance. The flight path and estimation routines were modified such that the velocity within each group was random, but velocities higher than a particle's

Table 1. Neutron Source Spectrum

Energy (MeV)	Neutrons MeV-cm^2-Source Monitor	Energy (MeV)	Neutrons MeV-cm^2-Source Monitor
1.4972(+1)*	1.9028(+5)	4.2205(+0)	7.2509(+5)
1.4033(+1)	1.2747(+5)	4.0780(+0)	7.5378(+5)
1.3181(+1)	1.5294(+5)	3.9426(+0)	7.7656(+5)
1.2404(+1)	1.6977(+5)	3.8139(+0)	8.0688(+5)
1.1695(+1)	1.9602(+5)	3.6914(+0)	8.5540(+5)
1.1045(+1)	2.1688(+5)	3.5747(+0)	8.1327(+5)
1.0448(+1)	2.3977(+5)	3.4635(+0)	8.4481(+5)
9.8985(+0)	2.6076(+5)	3.3574(+0)	9.2436(+5)
9.3914(+0)	2.8350(+5)	3.2561(+0)	8.7982(+5)
8.9225(+0)	3.1491(+5)	3.1593(+0)	8.6795(+5)
8.4880(+0)	3.3893(+5)	3.0668(+0)	9.2082(+5)
8.0846(+0)	3.5023(+5)	2.9783(+0)	9.4133(+5)
7.7094(+0)	3.6188(+5)	2.8936(+0)	9.0987(+5)
7.3599(+0)	3.9201(+5)	2.8124(+0)	8.7041(+5)
7.0337(+0)	4.0031(+5)	2.7347(+0)	9.0445(+5)
6.7287(+0)	4.3024(+5)	2.6601(+0)	1.0602(+6)
6.4433(+0)	4.6726(+5)	2.5885(+0)	1.3765(+6)
6.1757(+0)	4.8543(+5)	2.5198(+0)	1.5363(+6)
5.9245(+0)	4.9031(+5)	2.4537(+0)	1.5228(+6)
5.6883(+0)	4.9696(+5)	2.3903(+0)	1.7013(+6)
5.4660(+0)	4.9298(+5)	2.3293(+0)	1.8020(+6)
5.2566(+0)	5.8466(+5)	2.2706(+0)	1.9321(+6)
5.0590(+0)	5.6452(+5)	2.2140(+0)	2.0422(+6)
4.8723(+0)	5.9045(+5)	2.1596(+0)	2.0729(+6)
4.6959(+0)	6.6819(+5)	2.1072(+0)	1.9707(+6)
4.5288(+0)	6.9952(+5)	2.0566(+0)	2.3224(+6)
4.3706(+0)	7.1198(+5)		

*Read as 1.4972×10^1.

Table 2. Energy Group Structure and Detector Response Functions

Group Number	Upper Energy (eV)	Neutron Response (Count/Neutron/cm^2)	Gamma Ray Response (Count/Gamma Ray/cm^2)	Neutron Induced Gamma Ray (Gamma Ray Count/Incident Neutron)
1	1.7333(+7)*	1.3900(-1)	0.0	5.8000(-3)
2	1.6487(+7)	1.3800(-1)	0.0	5.1000(-3)
3	1.5683(+7)	1.3700(-1)	0.0	5.9000(-3)
4	1.4918(+7)	1.3700(-1)	0.0	6.2000(-3)
5	1.4550(+7)	1.3800(-1)	0.0	6.4000(-3)
6	1.4191(+7)	1.3800(-1)	0.0	6.5000(-3)
7	1.3840(+7)	1.3900(-1)	0.0	7.0000(-3)
8	1.3499(+7)	1.4100(-1)	0.0	7.5000(-3)
9	1.2840(+7)	1.4400(-1)	0.0	8.0000(-3)
10	1.2214(+7)	1.4600(-1)	0.0	8.5000(-3)
11	1.1618(+7)	1.4800(-1)	0.0	9.2000(-3)
12	1.1052(+7)	1.5000(-1)	0.0	9.2000(-3)
13	1.0513(+7)	1.5100(-1)	0.0	9.0000(-3)
14	1.0000(+7)	1.5300(-1)	0.0	8.5000(-3)
15	9.5123(+6)	1.5600(-1)	0.0	8.3000(-3)
16	9.0484(+6)	1.5800(-1)	0.0	8.1000(-3)
17	8.6071(+6)	1.6200(-1)	0.0	8.2000(-3)
18	8.1873(+6)	1.6800(-1)	0.0	8.3000(-3)
19	7.7880(+6)	1.7500(-1)	0.0	8.0000(-3)
20	7.4082(+6)	1.8100(-1)	0.0	7.1000(-3)
21	7.0469(+6)	1.8700(-1)	0.0	5.7000(-3)
22	6.7032(+6)	1.9100(-1)	0.0	5.7000(-3)
23	6.5924(+6)	1.9400(-1)	0.0	6.0000(-3)
24	6.3763(+6)	1.9900(-1)	0.0	6.2000(-3)
25	6.0653(+6)	2.0400(-1)	0.0	5.7000(-3)
26	5.7695(+6)	2.0900(-1)	0.0	5.6000(-3)
27	5.4881(+6)	2.1300(-1)	0.0	5.0000(-3)
28	5.2205(+6)	2.1900(-1)	0.0	4.5000(-3)
29	4.9659(+6)	2.2300(-1)	0.0	4.0000(-3)
30	4.7237(+6)	2.2700(-1)	0.0	3.5000(-3)
31	4.4938(+6)	2.3400(-1)	0.0	3.1000(-3)
32	4.0657(+6)	2.3900(-1)	0.0	2.5000(-3)
33	3.6788(+6)	2.4600(-1)	0.0	2.1000(-3)
34	3.3287(+6)	2.5100(-1)	0.0	1.7000(-3)
35	3.1664(+6)	2.5300(-1)	0.0	1.6000(-3)
36	3.0119(+6)	2.5700(-1)	0.0	1.5000(-3)
37	2.8650(+6)	2.6000(-1)	0.0	1.4000(-3)
38	2.7253(+6)	2.6200(-1)	0.0	1.3000(-3)
39	2.5924(+6)	2.6500(-1)	0.0	1.5000(-3)
40	2.4660(+6)	2.6700(-1)	0.0	1.1000(-3)

Table 2. Continued

41	2.3852(+6)	2.6800(-1)	0.0	1.1000(-3)
42	2.3653(+6)	2.6900(-1)	0.0	1.1000(-3)
43	2.3457(+6)	2.6900(-1)	0.0	1.1000(-3)
44	2.3069(+6)	2.6900(-1)	0.0	1.1000(-3)
45	2.2313(+6)	2.7000(-1)	0.0	1.0000(-3)
46	2.1225(+6)	2.6900(-1)	0.0	9.0000(-4)
47	2.0190(+6)	2.6800(-1)	0.0	7.7000(-4)
48	1.9205(+6)	2.6700(-1)	0.0	6.5000(-4)
49	1.8268(+6)	2.6500(-1)	0.0	6.3000(-4)
50	1.7377(+6)	2.6300(-1)	0.0	5.5000(-)
51	1.6530(+6)	2.6200(-1)	0.0	4.8000(-4)
52	1.5724(+6)	2.5700(-1)	0.0	4.0000(-4)
53	1.4957(+6)	2.5300(-1)	0.0	3.7000(-4)
54	1.4227(+6)	2.4700(-1)	0.0	3.2000(-4)
55	1.3534(+6)	2.3500(-1)	0.0	2.8000(-4)
56	1.2873(+6)	2.2900(-1)	0.0	2.3000(-4)
57	1.2246(+6)	2.2200(-1)	0.0	2.0000(-4)
58	1.1648(+6)	1.9400(-1)	0.0	1.6000(-4)
59	1.1080(+6)	1.6000(-1)	0.0	1.1000(-4)
60	1.0026(+6)	1.3100(-1)	0.0	1.1000(-4)
61	9.6164(+5)	1.1100(-1)	0.0	1.1000(-4)
62	9.0718(+5)	9.1200(-2)	0.0	1.0800(-4)
63	8.6294(+5)	7.3600(-2)	0.0	1.0500(-4)
64	8.2085(+5)	5.6888(-2)	0.0	1.0300(-4)
65	7.8080(+5)	4.0900(-2)	0.0	1.0000(-5)
66	7.4274(+5)	2.5700(-2)	0.0	9.5000(-5)
67	7.0651(+5)	1.1200(-2)	0.0	9.0000(-5)
68	6.7206(+5)	8.0000(-3)	0.0	8.5000(-5)
69	6.3928(+5)	4.0000(-3)	0.0	8.0000(-5)
70	6.0810(+5)	2.0000(-4)	0.0	7.5000(-5)
71	5.7844(+5)	0.0	0.0	7.0000(-5)
72	5.5023(+5)	0.0	0.0	6.5000(-5)
73	5.2340(+5)	0.0	0.0	6.0000(-5)
74	4.9787(+5)	0.0	0.0	5.7000(-5)
75	4.5049(+5)	0.0	0.0	5.3000(-5)
76	4.0762(+5)	0.0	0.0	5.0000(-5)
77	3.8774(+5)	0.0	0.0	4.7000(-5)
78	3.6883(+5)	0.0	0.0	4.3000(-5)
79	3.3373(+5)	0.0	0.0	4.0000(-5)
80	3.0197(+5)	0.0	0.0	3.7000(-5)
81	2.9850(+5)	0.0	0.0	3.6000(-5)
82	2.9720(+5)	0.0	0.0	3.5000(-5)

Table 2. Continued

83	2.9452(+5)	0.0	0.0	3.4000(-5)
84	2.8725(+5)	0.0	0.0	3.3000(-5)
85	2.7324(+5)	0.0	0.0	3.2000(-5)
86	2.4724(+5)	0.0	0.0	3.1000(-5)
87	2.3518(+5)	0.0	0.0	3.0000(-5)
88	2.2371(+5)	0.0	0.0	2.9000(-5)
89	2.1280(+5)	0.0	0.0	2.8000(-5)
90	2.0242(+5)	0.0	0.0	2.7000(-5)
91	1.9255(+5)	0.0	0.0	2.6500(-5)
92	1.8316(+5)	0.0	0.0	2.6000(-5)
93	1.7422(+5)	0.0	0.0	2.5500(-5)
94	1.6573(+5)	0.0	0.0	2.5000(-5)
95	1.5764(+5)	0.0	0.0	2.4500(-5)
96	1.4996(+5)	0.0	0.0	2.4000(-5)
97	1.4264(+5)	0.0	0.0	2.3500(-5)
98	1.3569(+5)	0.0	0.0	2.3000(-5)
99	1.2907(+5)	0.0	0.0	2.2500(-5)
100	1.2277(+5)	0.0	0.0	2.2000(-5)
101	1.1679(+5)	0.0	0.0	2.1500(-5)
102	1.1109(+5)	0.0	0.0	2.1100(-5)
103	9.8037(+4)	0.0	0.0	2.1000(-5)
104	8.6517(+4)	0.0	0.0	2.1000(-5)
105	8.2500(+4)	0.0	0.0	2.2000(-5)
106	7.9500(+4)	0.0	0.0	2.2000(-5)
107	7.2000(+4)	0.0	0.0	2.3000(-5)
108	6.7379(+4)	0.0	0.0	2.6000(-5)
109	5.6562(+4)	0.0	0.0	2.7000(-5)
110	5.2475(+4)	0.0	0.0	2.8000(-5)
111	4.6309(+4)	0.0	0.0	2.9000(-5)
112	4.0868(+4)	0.0	0.0	3.0000(-5)
113	3.4307(+4)	0.0	0.0	3.2000(-5)
114	3.1828(+4)	0.0	0.0	3.4000(-5)
115	2.8500(+4)	0.0	0.0	3.5000(-5)
116	2.7000(+4)	0.0	0.0	3.6000(-5)
117	2.6058(+4)	0.0	0.0	3.7000(-5)
118	2.4788(+4)	0.0	0.0	3.8000(-5)
119	2.4176(+4)	0.0	0.0	3.9000(-5)
120	2.3579(+4)	0.0	0.0	4.0000(-5)
121	2.1875(+4)	0.0	0.0	4.7000(-5)
122	1.9305(+4)	0.0	0.0	5.3000(-5)
123	1.5034(+4)	0.0	0.0	6.0000(-5)
124	1.1709(+4)	0.0	0.0	6.3000(-5)
125	9.1188(+3)	0.0	0.0	7.0000(-5)
126	7.1017(+3)	0.0	0.0	7.2000(-5)

Table 2. Continued

127	5.5308(+3)	0.0	0.0	7.0000(-5)
128	4.3074(+3)	0.0	0.0	6.8000(-5)
129	3.7074(+3)	0.0	0.0	6.5000(-5)
130	3.3546(+3)	0.0	0.0	6.2000(-5)
131	3.0324(+3)	0.0	0.0	6.0000(-5)
132	2.7465(+3)	0.0	0.0	5.8000(-5)
133	2.6126(+3)	0.0	0.0	5.5000(-5)
134	2.4852(+3)	0.0	0.0	5.4000(-5)
135	2.2487(+3)	0.0	0.0	5.2000(-5)
136	2.0347(+3)	0.0	0.0	5.0000(-5)
137	1.5846(+3)	0.0	0.0	4.5000(-5)
138	1.2341(+3)	0.0	0.0	4.3000(-5)
139	9.6112(+2)	0.0	0.0	4.7000(-5)
140	7.4852(+2)	0.0	0.0	5.0000(-5)
141	5.8295(+2)	0.0	0.0	5.3000(-5)
142	4.5400(+2)	0.0	0.0	5.5000(-5)
143	3.5358(+2)	0.0	0.0	6.5000(-5)
144	2.7536(+2)	0.0	0.0	7.5000(-5)
145	2.1445(+2)	0.0	0.0	8.5000(-5)
146	1.6702(+2)	0.0	0.0	1.0000(-4)
147	1.3007(+2)	0.0	0.0	1.2000(-4)
148	1.0130(+2)	0.0	0.0	1.3700(-4)
149	7.8893(+1)	0.0	0.0	1.5400(-4)
150	6.1442(+1)	0.0	0.0	1.7400(-4)
151	4.7851(+1)	0.0	0.0	1.9500(-4)
152	3.7267(+1)	0.0	0.0	2.2000(-4)
153	2.9023(+1)	0.0	0.0	2.4800(-4)
154	2.2603(+1)	0.0	0.0	2.7900(-4)
155	1.7603(+1)	0.0	0.0	3.1400(-4)
156	1.3710(+1)	0.0	0.0	3.5300(-4)
157	1.0677(+1)	0.0	0.0	3.9700(-4)
158	8.3153	0.0	0.0	4.4700(-4)
159	6.4760	0.0	0.0	5.0400(-4)
160	5.0435	0.0	0.0	5.6700(-4)
161	3.9279	0.0	0.0	6.3800(-4)
162	3.0590	0.0	0.0	7.1800(-4)
163	2.3824	0.0	0.0	8.0800(-4)
164	1.8554	0.0	0.0	9.1000(-4)
165	1.4450	0.0	0.0	1.0200(-3)
166	1.1254	0.0	0.0	1.1500(-3)
167	8.7642(-1)	0.0	0.0	1.3000(-3)
168	6.8256(-1)	0.0	0.0	1.4600(-3)
169	5.3156(-1)	0.0	0.0	1.6400(-3)
170	4.1399(-1)	0.0	0.0	2.1900(-3)

Table 2. Continued

171	1.0000(-1)**	0.0	0.0	4.7600(-3)
172	1.4000(+7)	0.0	1.1900(-1)	0.0
173	1.2000(+7)	0.0	1.1500(-1)	0.0
174	1.0000(+7)	0.0	1.1500(-1)	0.0
175	8.0000(+6)	0.0	1.1200(-1)	0.0
176	7.5000(+6)	0.0	1.1200(-1)	0.0
177	7.0000(+6)	0.0	1.1200(-1)	0.0
178	6.5000(+6)	0.0	1.1200(-1)	0.0
179	6.0000(+6)	0.0	1.1200(-1)	0.0
180	5.5000(+6)	0.0	1.1200(-1)	0.0
181	5.0000(+6)	0.0	1.1200(-1)	0.0
182	4.5000(+6)	0.0	1.1200(-1)	0.0
183	4.0000(+6)	0.0	1.1300(-1)	0.0
184	3.5000(+6)	0.0	1.1300(-1)	0.0
185	3.0000(+6)	0.0	1.1400(-1)	0.0
186	2.5000(+6)	0.0	1.1300(-1)	0.0
187	2.0000(+6)	0.0	1.0900(-1)	0.0
188	1.6600(+6)	0.0	1.0800(-1)	0.0
189	1.5000(+6)	0.0	1.0500(-1)	0.0
190	1.3300(+6)	0.0	9.3000(-2)	0.0
191	1.0000(+6)	0.0	7.0000(-2)	0.0
192	8.0000(+5)	0.0	3.7000(-2)	0.0
193	7.0000(+5)	0.0	1.1000(-2)	0.0
194	6.0000(+5)	0.0	0.0	0.0
195	5.1200(+5)	0.0	0.0	0.0
196	5.1000(+5)	0.0	0.0	0.0
197	4.5000(+5)	0.0	0.0	0.0
198	4.0000(+5)	0.0	0.0	0.0
199	3.0000(+5)	0.0	0.0	0.0
200	2.0000(+5)	0.0	0.0	0.0
201	1.5000(+5)	0.0	0.0	0.0
202	1.0000(+5)	0.0	0.0	0.0
203	7.5000(+4)	0.0	0.0	0.0
204	6.0000(+4)	0.0	0.0	0.0
205	4.5000(+4)	0.0	0.0	0.0
206	3.0000(+4)	0.0	0.0	0.0
207	2.0000(+4)***	0.0	0.0	0.0

*Read as 1.7333×10^{7}.

**Lowest neutron energy is 1.0000(-5).

***Lowest gamma ray energy is 1.0000(+4).

Table 3. Material Compositions in atoms/barn-cm

Concrete		Steel	
Element	Concentration	Element	Concentration
Hydrogen	7.680(-3)	Carbon	2.360(-4)
Oxygen	4.350(-2)	Manganese	3.440(-4)
Sodium	4.000(-5)	Iron	8.427(-2)
Magnesium	2.200(-4)		
Aluminum	6.400(-4)		
Silicon	1.741(-2)		
Potassium	2.500(-4)		
Calcium	2.870(-3)		
Iron	2.600(-4)		
Sulfur	8.000(-5)		

initial velocity were not allowed. The Russian roulette and splitting games were modified such that they were applied at the boundaries between the sections of the slab rather than at each collision. The parameters for these processes were updated in a continuous fashion rather than being set by input data. At each boundary all parameters were modified by e^{Kz} where K was chosen as 0.06 and z is the distance from the source plane to the boundary, parallel to the axis of the slab.

For the neutrons, the standard next event estimator from source and collision events was used. For the secondary gamma rays, the estimation was performed using the Klein-Nishina formulation.[5] The calculation was done in the MORSE primary particle mode, and the necessary checks were inserted into the random walk and estimation processes to distinguish between neutrons and gamma rays.

The calculated count rates and flux spectra were collected in the time and energy intervals given in Tables 4 and 5. In Table 4 the energies are

Table 4. Time Interval Limits

Time (μsec)	Corresponding Energy (MeV)
0.995	15.0
1.110	12.0
1.214	10.0
1.279	9.0
1.355	8.0
1.448	7.0
1.562	6.0
1.710	5.0
1.911	4.0
2.204	3.0
2.413	2.5
2.544	2.25
2.698	2.0

Table 5. Flux Spectra Energy Intervals

Group Number	Upper Energy (MeV)	Group Number	Upper Energy (MeV)
2	16.49	74	0.9616
4	15.68	102	0.4505*
6	14.55	172	14.0
8	13.84	173	12.0
10	12.84	174	10.0
12	11.62	176	8.0
14	10.51	178	7.0
16	9.512	180	6.0
18	8.607	182	5.0
21	7.788	184	4.0
25	6.703	186	3.0
29	5.770	190	2.0
32	4.724	194	1.0**
36	3.379		
47	2.865		
60	1.921		

*Lower neutron energy is 0.045 MeV.

**Lower gamma-ray energy is 0.512 MeV.

given which correspond to the arrival time at the leading edge of the slab from the source. In order to compare the calculated flux spectra with the measured data, the calculated data was given a Gaussian energy smear using parameters provided with the experimental data in reference 1. This process, done external to the MORSE calculation, used the detector resolution function shown in Table 6 (FWHM is the Gaussian full width-half maximum in percent).

Table 6. Detector Resolution Function

	FWHM (%)	
Energy (MeV)	Neutrons	Gamma Rays
0.0	50.0	50.0
0.9	50.0	50.0
1.33	50.0	40.0
1.78	50.0	34.9
2.1	44.6	32.0
2.5	40.0	29.4
3.0	35.7	26.7
3.5	32.4	24.6
4.0	29.8	23.0
5.0	26.2	20.8
6.0	23.6	18.9
7.0	21.7	17.6
9.0	18.9	15.5
12.0	16.3	13.6
16.0	14.1	12.0

IV. PRESENTATION OF RESULTS

Comparison of the measured and calculated data for the 0.995-2.698 μsec time interval (15-2 MeV energy interval) are given in Figs. 3-16. Neutron and secondary gamma-ray count rates are plotted as a function of time in Fig. 3. Neutron spectral results are shown in Figs. 4-13, with each plot corresponding to a different incident neutron energy range. The gamma-ray spectral results in Figs. 14-16 correspond to three broad ranges of incident neutron energy. These results are correlated, i.e., they are all from one MORSE calculation. Each error bar represents plus or minus one standard deviation from the mean calculated value. The two curves of the experimental spectra also represents plus or minus one standard deviation from the mean measured value. The calculated spectra have been given a detector resolution smear as indicated in the previous section. The gamma-ray count rates in Fig. 3 contain the contributions from the neutron induced gamma-ray counts in the detector, amounting to only a few percent for each time interval. However, this contribution has not been included in the gamma-ray spectra because information about the energy of these neutron induced gamma rays was not provided. In Fig. 3 the time scale represents the particle detection time at the detector with time zero at the source point at the far end of the flight path. The incident energies given at the top of the figure correspond to the energy of the neutron whose time is given on the bottom scale. One flux spectrum plot is given for each incident energy interval. Due to an unexplained inconsistency in the reported measured data, the calculated neutron spectra have been multiplied by 15.74 in order to be compared with the experimental data.[5] No such adjustment was necessary for the count rates or gamma-ray spectra.

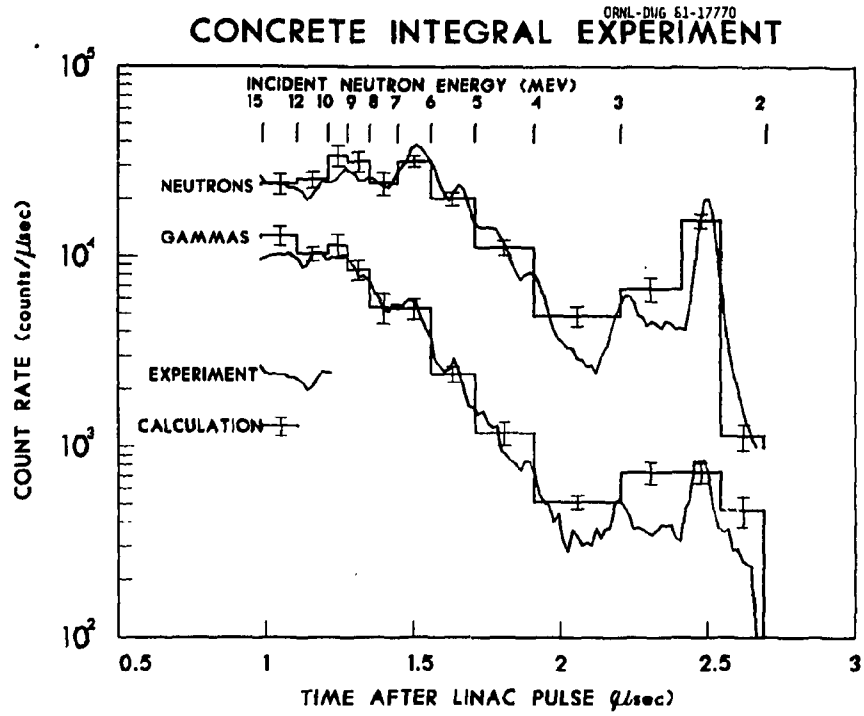

Fig. 3. Neutron and Secondary Gamma-Ray Count-Rate Comparisons.

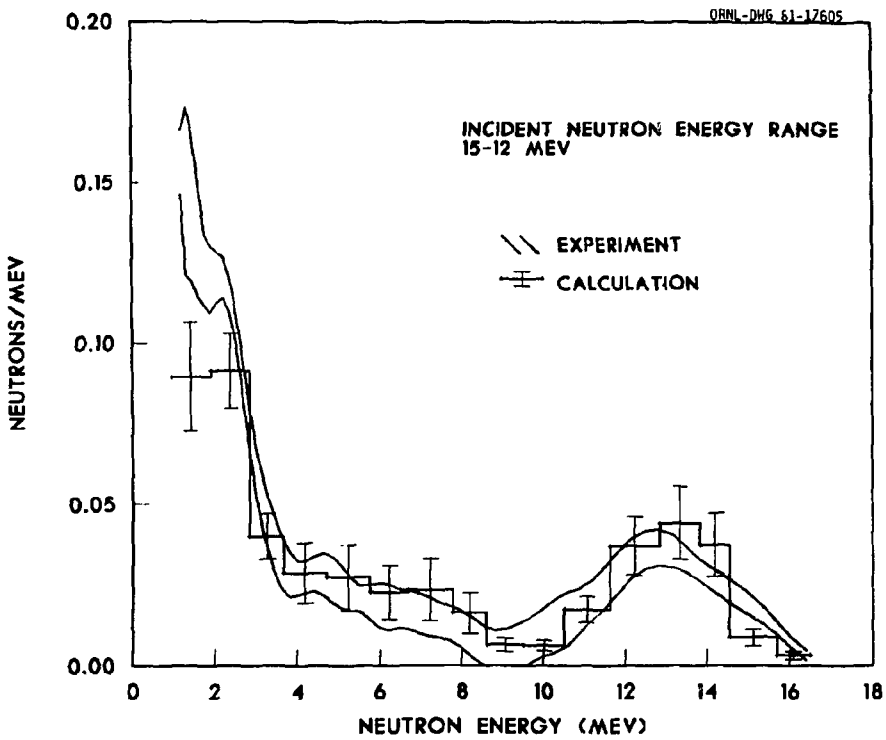

Fig. 4. Neutron Energy Spectrum for the 15-12 MeV Energy Interval.

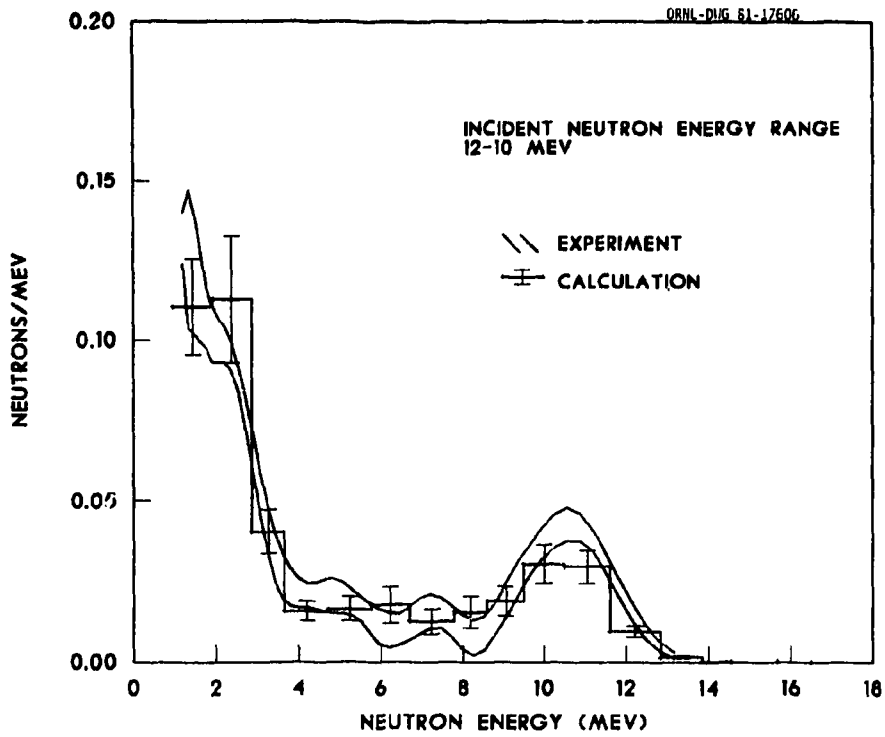

Fig. 5. Neutron Energy Spectrum for the 12-10 MeV Energy Interval.

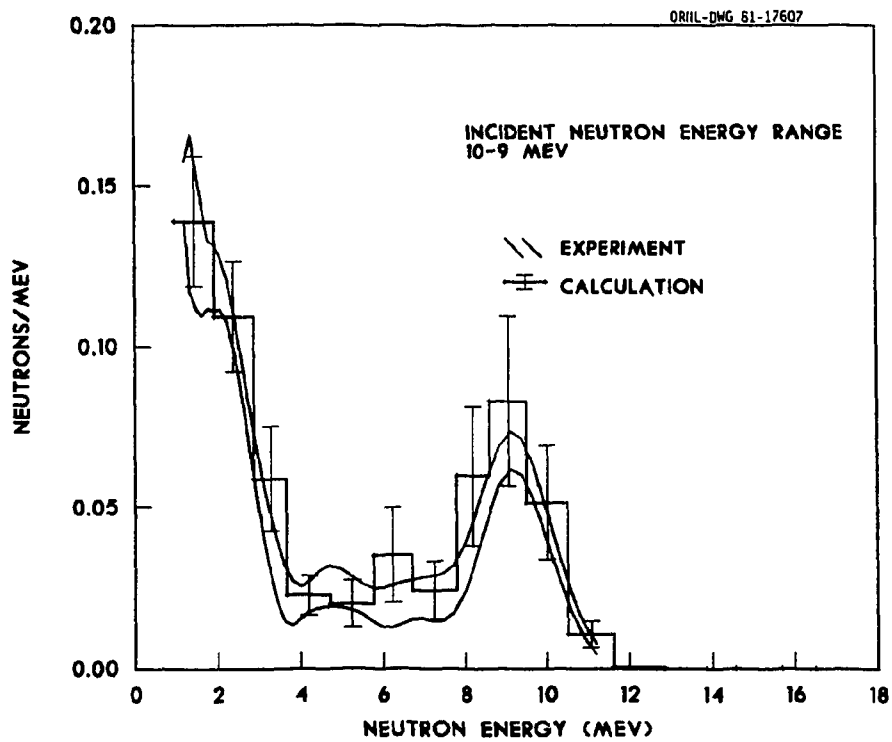

Fig. 6. Neutron Energy Spectrum for the 10-9 MeV Energy Interval.

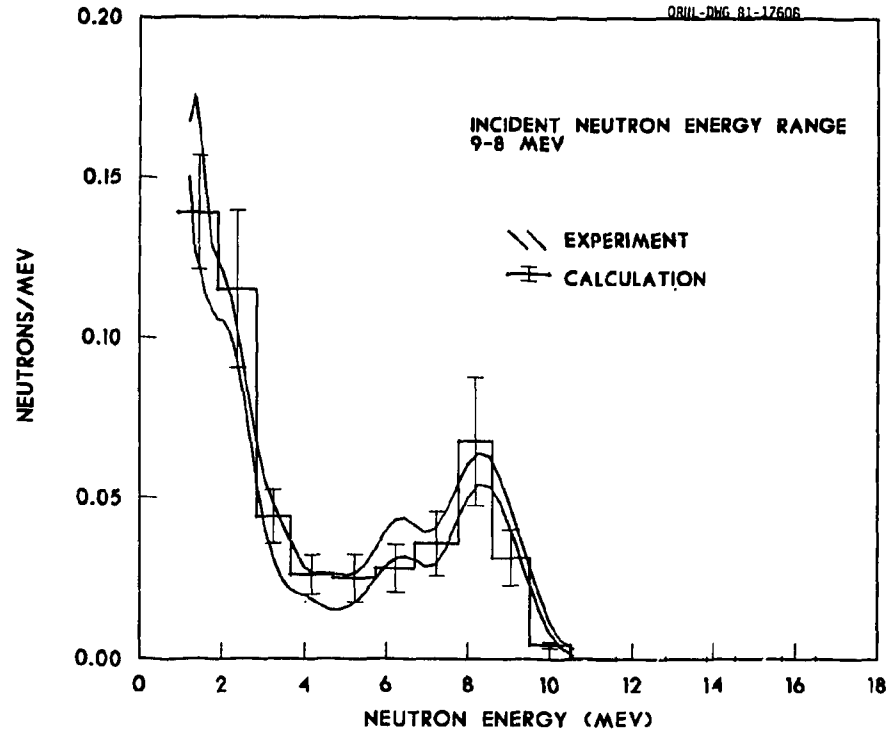

Fig. 7. Neutron Energy Spectrum for the 9-8 MeV Energy Interval.

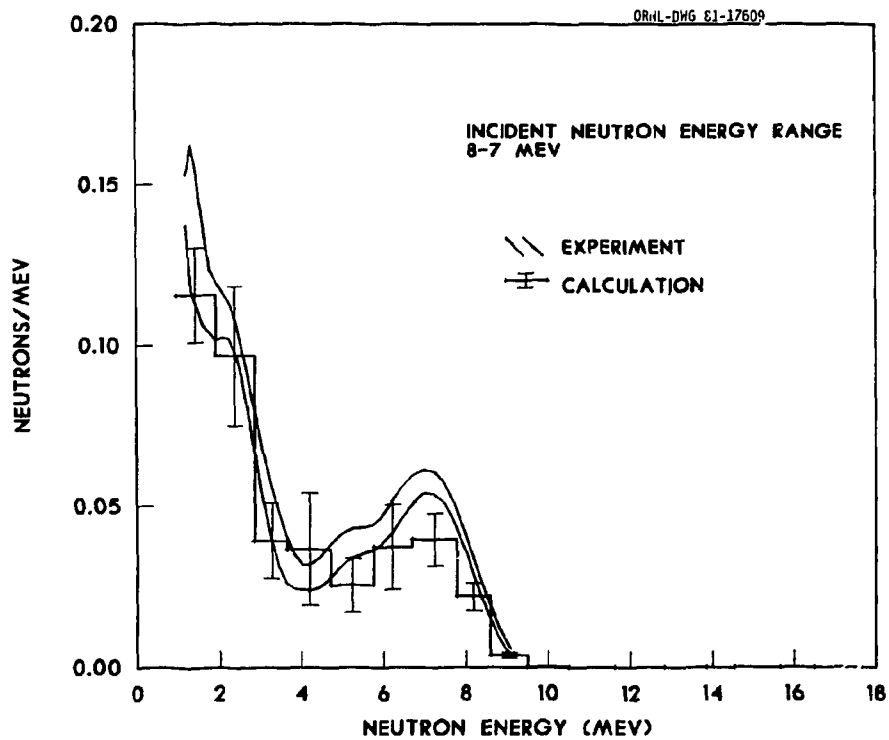

Fig. 8. Neutron Energy Spectrum for the 8-7 MeV Energy Interval.

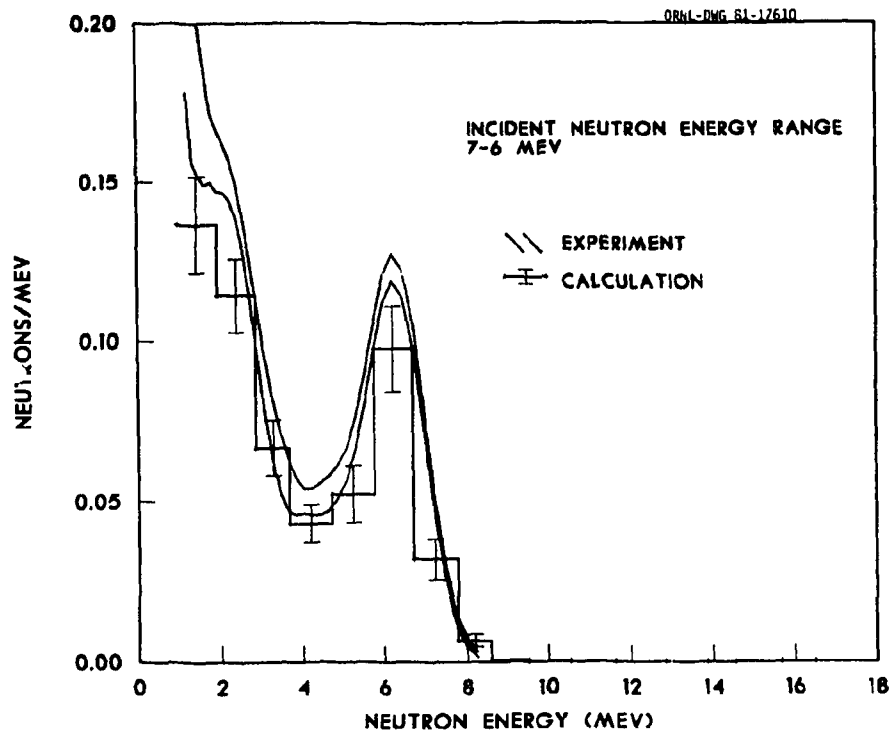

Fig. 9. Neutron Energy Spectrum for the 7-6 MeV Energy Interval.

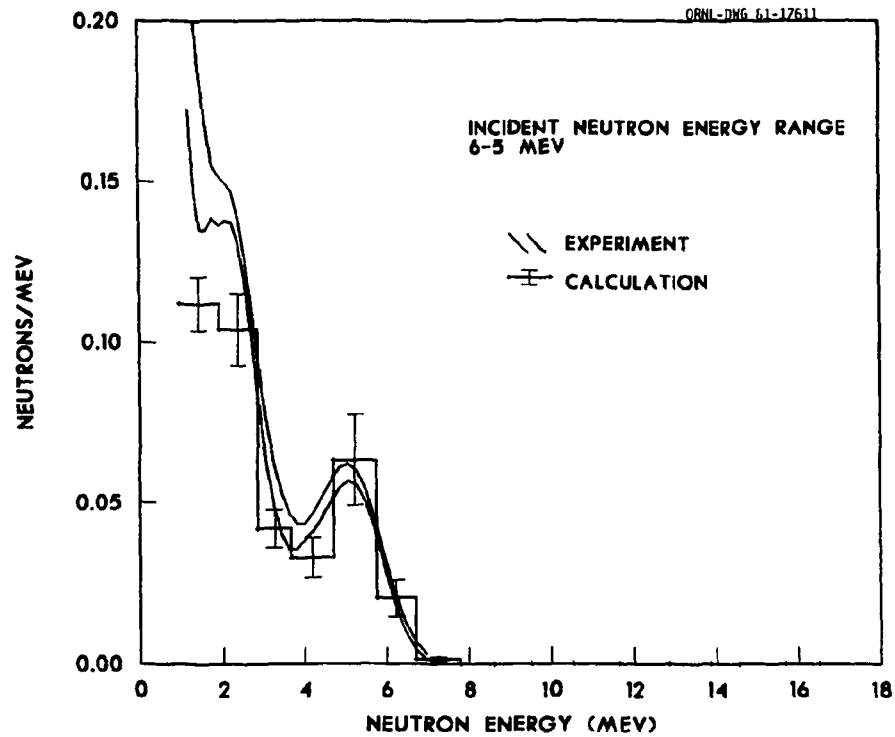

Fig. 10. Neutron Energy Spectrum for the 6-5 MeV Energy Interval.

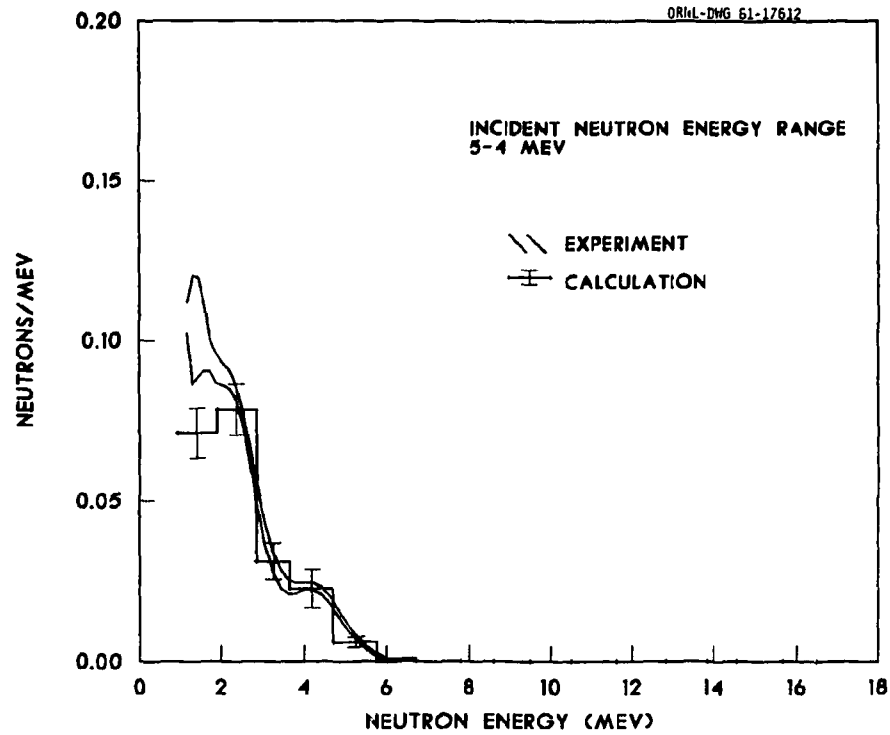

Fig. 11. Neutron Energy Spectrum tor the 5-4 MeV Energy Interval.

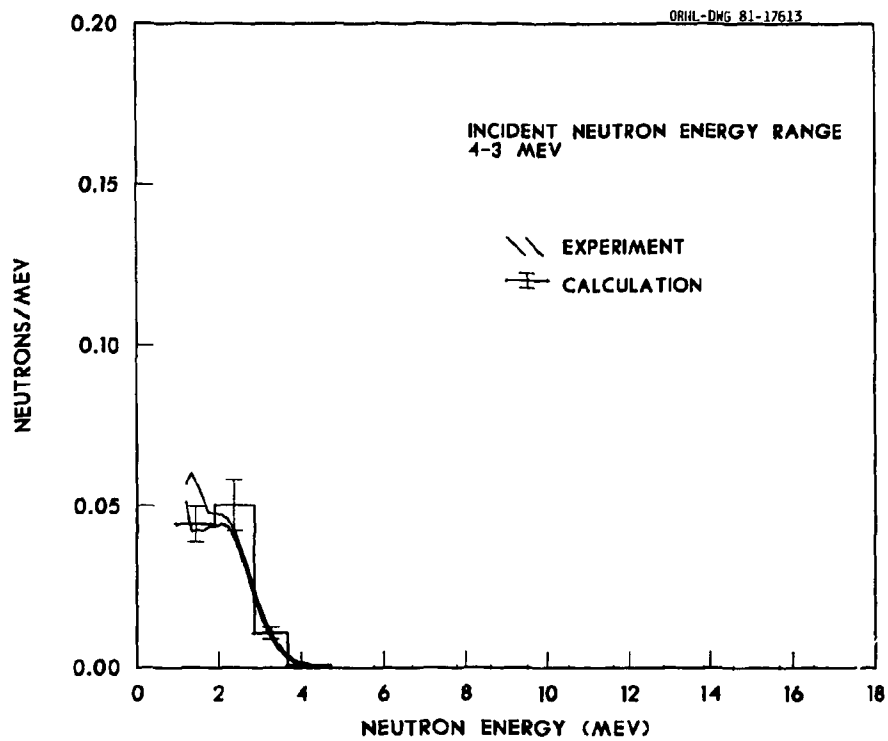

Fig. 12. Neutron Energy Spectrum for the 4-3 MeV Energy Interval.

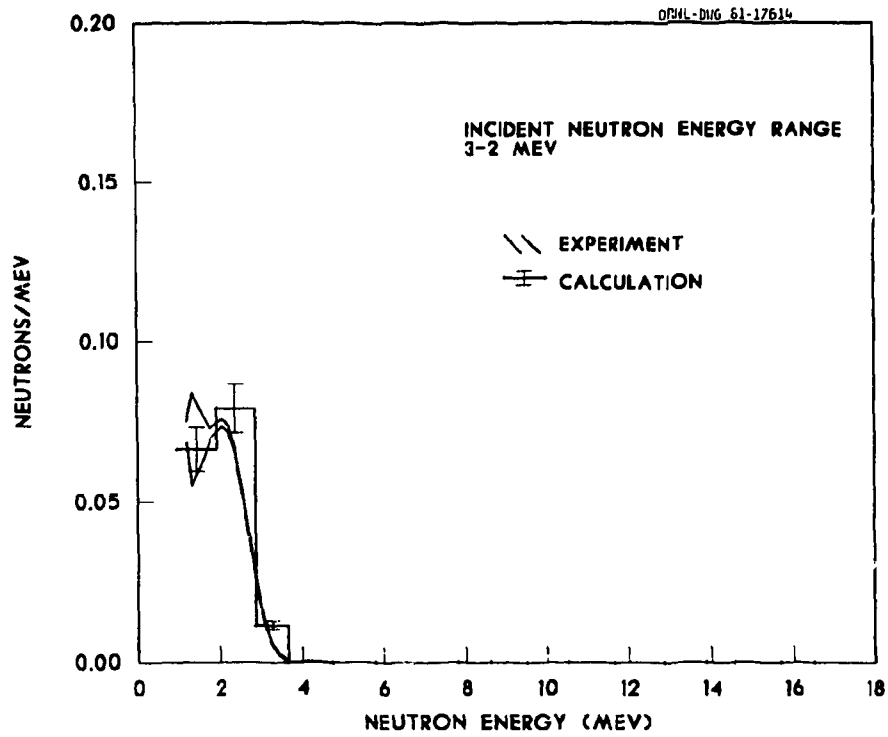

Fig. 13. Neutron Energy Spectrum for the 3-2 MeV Energy Interval.

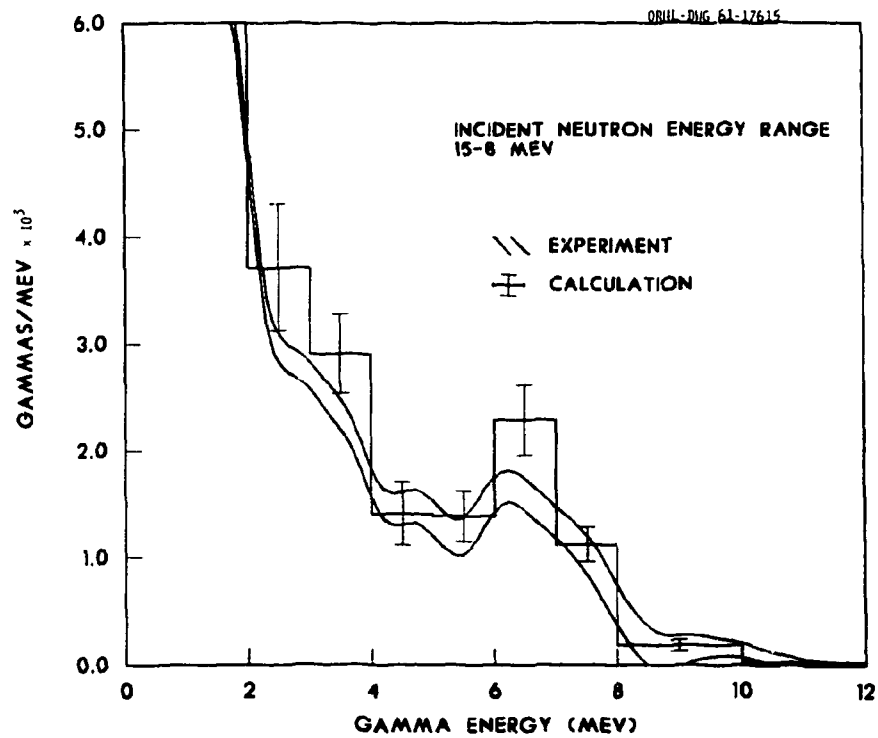

Fig. 14. Secondary Gamma-Ray Spectrum for the 15-8 MeV Incident Neutron Energy Interval.

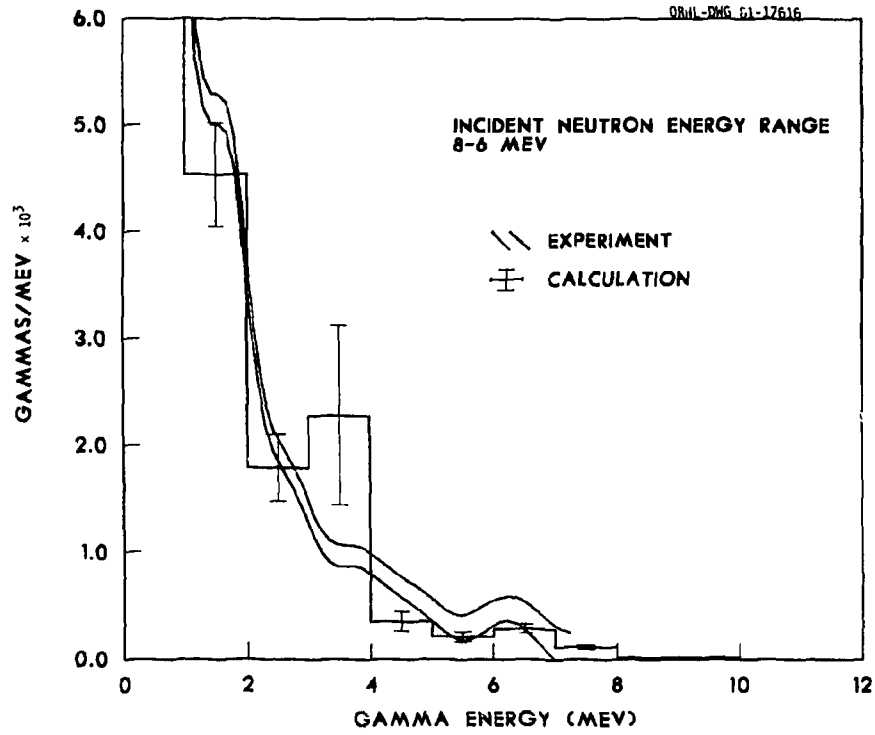

Fig. 15. Secondary Gamma-Ray Spectrum for the 8-6 MeV Incident Neutron Energy Interval.

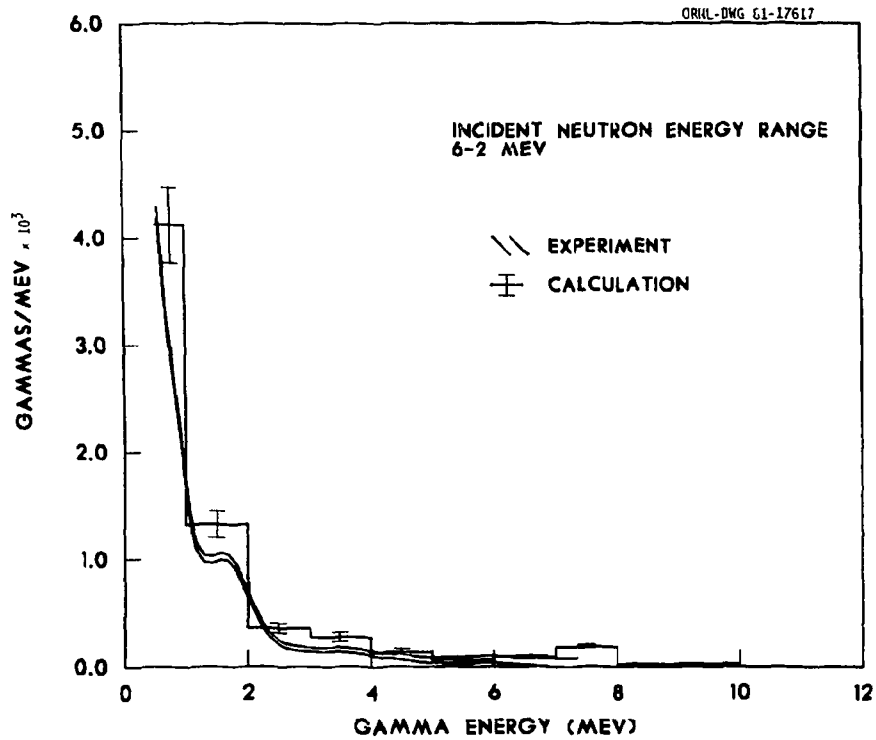

Fig. 16. Secondary Gamma-Ray Spectrum for the 6-2 MeV Incident Neutron Energy Interval.

The neutron count rate comparisons (Fig. 3) are in good general agreement except in the 2-2.5 μsec time interval where the calculated count rate is high. This effect also causes the secondary gamma-ray count to be high in the same time interval. It is seen that the neutron spectra (Figs. 4-13) are also in good general agreement. In only a few cases is the error bar of the calculated value outside of the spread of the measured data, although the statistical uncertainty of the calculated data sometimes exceeds 30% of its mean value.

It is noted that in the neutron spectrum comparison shown in Fig. 4 (15-12 MeV range), the lowest energy calculated results between 1 and 3 Mev are much lower than the measured data. It was found from additional calculations that this effect is due to the lack of the inclusion in the calculation of source neutrons above 15 MeV (see Table 1). In the remaining neutron spectrum comparisons a significant portion of the flux in the two low energy histograms comes from neutrons in a higher incident energy interval (earlier time interval) that have scattered into the current interval, violating the assumption of exact time-energy correlation in creating these spectrum comparisons. It is noted that this low energy spectrum effect is much more pronounced in the calculated results from the TRIPOLI code,[6] although these comparisons in general are superior to the MORSE results given here. The TRIPOLI results are not from a true time-dependent calculation, but from a separate energy-dependent calculation for each incident-energy interval, utilizing the time-energy correlation of the neutrons in the flight path. Thus the low-energy spectra for each interval in the TRIPOLI results are due to there being no contributions from higher

incident energy intervals, and not as a result of the detector resolution smearing technique as suggested in reference 6.

Preliminary calculations with the standard DNA 37-21 group cross-section library[7] proved woefully inadequate, especially for the flux spectrum comparisons, due to lack of detail in the group structure. The high energy peak for each interval was greatly underpredicted, and in some cases, such as at 6 MeV in the 7-6 MeV interval, there was no peak at all. It is possible that even with the 171-36 VITAMIN C library a higher order expansion than P_3 would have improved the results presented here.

For neutron spectral result comparisons with the measured data, energy-dependent calculations are adequate. However, to correctly compare gamma-ray results, true time-dependent calculations are necessary to obtain the correct source of secondary gamma rays in each time and energy interval. Although there are several poorly calculated points in the gamma-ray spectra in Figs. 14-16, the general comparisons with the measured data are acceptable, particularly with regard to shape. The incident neutron energy intervals are so wide that it is difficult to isolate specific cross-section data for examination. The 6-2 MeV interval spectrum does not reflect the high calculated values in the count rate curve, and the difference must be due to the energy dependence of the response function (see Table 2).

V. CONCLUSIONS

The calculations presented here give good general comparisons with the measured data of reference 1. To calculate time and differential energy-dependent results for neutrons and secondary gamma rays traversing a meter

of steel and concrete is not a particularly straight forward task. It was necessary to employ a large cross-section data set, and the P_3 expansion may still be inadequate. Several necessary non-standard procedures were programmed into the MORSE code. Efforts are continuing in several areas concerning this experiment. Of particular interest is the calculation of the time-dependent thermal neutron capture. This effect is of primary importance in making comparisons with the measured long-time gamma-ray data where any original time-energy correlation of the incident neutrons has been lost.

REFERENCES

1. J. C. Young et al., "Time-Dependent Measurements of Fast-Neutron and Secondary Gamma-Ray Transport Through a Thick Concrete and Steel Shield," IRT 8025-723, IRT Corporation (1975).

2. M. B. Emmett, "The Morse Monte Carlo Radiation Transport Code System," ORNL/TM-4972 (1975). Available from the Radiation Shielding Information Center (RSIC) at Oak Ridge National Laboratory (ORNL) as CCC-203/MORSE-CG.

3. R. W. Roussin, C. R. Weisbin, J. E. White, N. M. Greene, R. Q. Wright, and J. B. Wright, "VITAMIN-C: The CTR Processed Multigroup Cross-Section Library for Neutronics Studies," ORNL/RSIC-37 (ENDF-296) (1980). Available from RSIC as DLC-41/VITAMIN-C.

4. A. Baur et al., "TRIPOLI II, Three-Dimensional Polyenergetic Monte Carlo Radiation Transport Program," (1980). Available from RSIC as CCC-372/TRIPOLI-II.

5. S. N. Cramer, "Adjoint Gamma Ray Estimation to the Surface of a Cylinder-Analysis of a Remote Reprocessing Facility," ORNL/TM-7686, Oak Ridge National Laboratory (1981).

6. S. N. Cramer and R. W. Roussin, "Experience with TRIPOLI at ORNL," presented in "A Review of the Theory and Application of Monte Carlo Methods," proceedings of a Seminar-Workshop, Oak Ridge, Tennessee, April 21-23, 1980, p. 295, ORNL/RSIC-44.

7. D. E. Bartine, J. R. Knight, J. V. Pace, III, and R. W. Roussin, "Production and Testing of the DNA Few Group Coupled Neutron-Gamma Cross-Section Library," ORNL/TM-4840 (1977). Available from RSIC as DLC-31/FEWG1.

INTERNAL DISTRIBUTION

1-5. L. S. Abbott
6. R. G. Alsmiller
7. D. E. Bartine
8. S. Bhuiyan
9-13. S. N. Cramer
14. M. B. Emmett
15. W. W. Engle, Jr.
16. G. F. Flanagan
17. T. A. Gabriel
18. H. Goldstein (Consultant)
19. T. J. Hoffman
20. R. A. Lillie
21. R. E. Maerker
22-26. F. C. Malenschein
27. J. F. Mincey
28. F. J. Muckenthaler
29. E. M. Oblow
30. J. V. Pace, III
31. R. W. Peelle
32-36. R. W. Roussin
37. J. C. Ryman
38. R. T. Santoro
39. C. O. Slater
40. J. S. Tang
41. D. K. Trubey
42. C. R. Weisbin
43. A. Zucker
44. P. W. Dickson, Jr. (Consultant)
45. H. J. C. Kouts (Consultant)
46. W. B. Lowenstein (Consultant)
47. R. Wilson (Consultant)
48-49. Central Research Library
50. Y-12 Document Ref. Section
51-52. Laboratory Records Dept.
53. Laboratory Records ORNL, RC
54. ORNL Patent Office
55-59. EPD Reports Office

EXTERNAL DISTRIBUTION

60. Office of the Assistant Manager for Energy Reseach & Development, DOE-ORO, Oak Ridge, TN 37830.

61-87. Technical Information Center (TIC).

88-155. Given DNA Transport Distribution.